IEEE Access
Multidisciplinary | Rapid Review | Open Access Journal

Received March 30, 2019, accepted April 25, 2019, date of publication May 6, 2019, date of current version May 17, 2019.

Digital Object Identifier 10.1109/ACCESS.2019.2914929

Real-Time Detection of Apple Leaf Diseases Using Deep Learning Approach Based on Improved Convolutional Neural Networks

PENG JIANG[1], YUEHAN CHEN[1], BIN LIU[1,2,3], DONGJIAN HE[2,3,4], AND CHUNQUAN LIANG[1,2]

[1]College of Information Engineering, Northwest A&F University, Yangling 712100, China
[2]Key Laboratory of Agricultural Internet of Things, Ministry of Agriculture and Rural Affairs, Northwest A&F University, Yangling 712100, China
[3]Shaanxi Key Laboratory of Agricultural Information Perception and Intelligent Service, Northwest A&F University, Yangling 712100, China
[4]College of Mechanical and Electronic Engineering, Northwest A&F University, Yangling 712100, China

Corresponding author: Bin Liu (liubin0929@nwsuaf.edu.cn)

This work was supported in part by the National Natural Science Foundation of China under Grant 61602388, in part by the China Postdoctoral Science Foundation under Grant 2017M613216, in part by the Postdoctoral Science Foundation of Shaanxi Province of China under Grant 2016BSHEDZZ121, in part by the Natural Science Basic Research Plan in Shaanxi Province of China under Grant 2017JM6059, in part by the National Natural Science Foundation of China under Grant 61402375, in part by the Natural Science Foundation of Hubei Province of China under Grant 2017CFB592, in part by the Fundamental Research Funds for the Central Universities under Grant 2452016081 and Grant 2452015194, and in part by the Innovation and Entrepreneurship Training Program of Northwest A&F University of China under Grant 2201810712291. *(Peng Jiang and Yuehan Chen are co-first authors.)*

ABSTRACT Alternaria leaf spot, Brown spot, Mosaic, Grey spot, and Rust are five common types of apple leaf diseases that severely affect apple yield. However, the existing research lacks an accurate and fast detector of apple diseases for ensuring the healthy development of the apple industry. This paper proposes a deep learning approach that is based on improved convolutional neural networks (CNNs) for the real-time detection of apple leaf diseases. In this paper, the apple leaf disease dataset (ALDD), which is composed of laboratory images and complex images under real field conditions, is first constructed via data augmentation and image annotation technologies. Based on this, a new apple leaf disease detection model that uses deep-CNNs is proposed by introducing the GoogLeNet Inception structure and Rainbow concatenation. Finally, under the hold-out testing dataset, using a dataset of 26,377 images of diseased apple leaves, the proposed INAR-SSD (SSD with Inception module and Rainbow concatenation) model is trained to detect these five common apple leaf diseases. The experimental results show that the INAR-SSD model realizes a detection performance of 78.80% mAP on ALDD, with a high-detection speed of 23.13 FPS. The results demonstrate that the novel INAR-SSD model provides a high-performance solution for the early diagnosis of apple leaf diseases that can perform real-time detection of these diseases with higher accuracy and faster detection speed than previous methods.

INDEX TERMS Apple leaf diseases, real-time detection, deep learning, convolutional neural networks, feature fusion.

I. INTRODUCTION

With a high nutritional and medicinal value, apples are one of the most productive types of fruit in the world. However, various diseases occur frequently on a large scale in apple production, thereby causing substantial economic losses. Therefore, the timely and effective detection of apple leaf diseases is crucial for ensuring the healthy development of the apple industry and has become a research hotspot in the field of agricultural information.

Traditionally, visual observation by experts has been conducted to diagnose plant diseases. However, there is a risk for error due to subjective perception [1]. In this context, various spectroscopic and imaging techniques have been studied for detecting plant diseases. However, they require precise instruments and bulky sensors [2], [3], which lead to high cost and low efficiency. In recent years, with the popularization of digital cameras and other electronic devices, automatic plant disease diagnosis via machine learning has been widely applied as a satisfactory alternative [4]–[11]. Nevertheless, in most cases, traditional machine learning approaches such as support vector machine (SVM) and K-means clustering have

The associate editor coordinating the review of this manuscript and approving it for publication was Huimin Lu.

complex image preprocessing and feature extraction steps, which reduce the efficiency of disease diagnosis. Machine learning approaches are more suitable for the identification of uniform-background plant images that have been captured in an ideal laboratory environment. Recently, deep learning and convolutional networks have made an essential breakthrough in computer vision and many relevant theoretical and practical achievements have been reported [12]–[14]. Because CNNs can extract features automatically and directly from the input images, thereby avoiding complex preprocessing on images, they have been a research hotspot in object detection [15], [16]. Inspired by the breakthroughs of CNNs in object detection, research and applications of CNNs are not rare in crop disease detection currently [17]–[23]. However, implementing the real-time detection of apple leaf diseases remains difficult because ALDD has the following characteristics: first, multiple diseases may occur on the same leaf. Moreover, the sizes of the disease spots on the leaves vary among diseases and for the same disease. In addition, most spots of apple leaf diseases are very small. Finally, environmental factors such as shadow, illumination, and soil also interfere with apple leaf disease detection.

To overcome these challenges, this paper applies the latest deep learning approach, which is based on improved convolutional neural networks, to perform real-time detection of apple leaf diseases. The main contributions of this paper are summarized as follows:

- The apple leaf disease dataset is built to provide an important guarantee of generalization capability of the proposed model. First, for enhancing the robustness of CNN model, diseased apple images with uniform and complex backgrounds are collected not only in the laboratory but also under real field conditions. Furthermore, to solve the problem that diseased apple leaf images are insufficient and prevent overfitting of the CNN-based model in the training process, natural diseased apple images are processed to generate sufficient training images via data augmentation technology.
- A novel real-time detection model that is based on the single-shot multibox detector (SSD) [24] for apple leaf diseases is proposed. First, the basic pre-network, namely, VGGNet [25], is modified to obtain the new basic pre-network, namely, VGG-INCEP (VGGNet with the Inception module) by introducing the GoogLeNet Inception module to improve the extraction performance for multiscale disease spots. Then, the Rainbow concatenation method in R-SSD [26] is integrated. Pooling and deconvolution are utilized simultaneously to integrate context and fuse features of the feature pyramid at the back of the SSD, via which higher small diseased object detection performance can be realized.
- A deep convolutional neural network is employed for the real-time detection of apple leaf diseases. The proposed deep-learning-based approach can automatically identify the discriminative features of the diseased apple images and detect the five common types of apple leaf diseases with high accuracy. At the same time, the proposed approach can detect not only various diseases in the same diseased image but also the same disease of different sizes in the same diseased image. In addition, the proposed approach can handle all the diseased apple images that were captured under real conditions in an apple field environment.

The experimental results demonstrate that the proposed real-time detection approach realizes a mean average precision of 78.80% and a detection speed of 23.13 FPS, which corresponds to an improvement of 2.98% mAP over the original SSD. The proposed model also exhibits strong detection performance and robustness.

The remainder of this paper is organized as follows: In Section II, generation techniques of ALDD are introduced briefly. Section III details the detection model for apple leaf diseases. In Section IV, experiments for evaluating the performance of the proposed approach are presented and the experimental results are analyzed. In Section V, related work is introduced and summarized. Finally, this paper is summarized in Section VI.

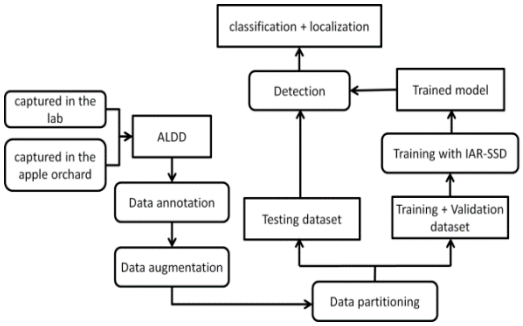

FIGURE 1. Real-time detection flow chart of apple leaf diseases.

II. GENERATING THE APPLE LEAF DISEASE DATASET

A. OVERVIEW

The detailed real-time detection process is illustrated in Figure 1. First, the ALDD is built by collecting diseased images from the laboratory and a real apple field. Then, the original ALDD is manually annotated and extended via a series of data augmentation operations. Next, the dataset is divided into two parts: The training dataset is used to train the INAR-SSD model and the testing dataset is used for performance evaluation. The detection results include both the classes and the locations of the identified apple leaf diseases.

B. APPLE LEAF DISEASE DATASET (ALDD)

1) DATA COLLECTION

At the beginning of our work, many human and material resources were devoted to the collection of diseased apple leaves because few suitable datasets were available for the real-time detection of apple leaf diseases. The disease patterns of apple leaves vary with the season and with other factors such as the humidity, temperature and illuminance.

For example, rainy weather is conducive to the generation and spread of germs, thereby resulting in the expansion and diffusion of the disease spots on affected leaves. Taking that into consideration, images of ALDD are collected under various weather conditions for more comprehensive applications. In addition to the artificially collected images, other images in the dataset are supplied by Apple Experiment Station of Northwest A&F University in Baishui county, Shaanxi province, China.

A total of 2029 images of diseased apple leaves are obtained, which correspond to five classes: Alternaria leaf spot (caused by Alternaria alternata f.sp mali), Brown spot (caused by Marssonina coronaria), Mosaic (caused by Papaya ringspot virus), Grey spot (caused by Phyllosticta pirina Sacc. and Coryneum foliicolum) and Rust (caused by Pucciniaceae glue rust). These five common diseases of apple leaves are selected for two reasons: initially, these five types of diseases can be visually identified from leaves, which is essential for the application of CNNs. In addition, they are responsible for substantial yield reductions in the apple industry.

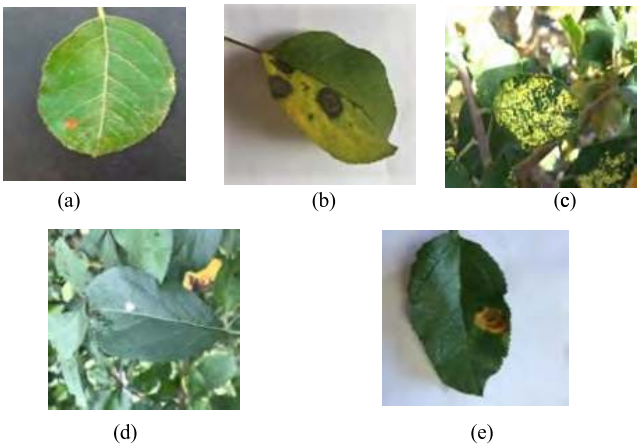

FIGURE 2. Five common types of apple leaf diseases. (a) Alternaria leaf spot. (b) Brown spot. (c) Mosaic. (d) Grey spot. (e) Rust.

Figure 2 shows representative images of the diseased apple leaves in the dataset. In Figure 2, the diversity among the five apple leaf diseases is easily observed. First, lesions that are caused by the same disease show certain commonalities under similar natural conditions. Second, the yellow lesions in the Mosaic class diffuse throughout the leaves, which distinguish them from other lesions. Third, the Alternaria leaf spot and Grey spot are similar in terms of geometric features, thereby increasing the complexity of detecting them. Finally, the Rust class is composed of rust-yellow spots that have brown pinhead-sized points in the center. Because of this remarkable difference, Rust is easier to distinguish from other diseases. These observations are helpful for the diagnosis and recognition of various apple leaf diseases.

The collected dataset has the following three characteristics: First, multiple diseases may co-occur on the same diseased image. Second, most images contain complex backgrounds, which ensures the high generalization performance of the approach. Finally, all diseased images in the dataset are annotated manually by experts.

2) IMAGE ANNOTATION

Image annotation is a vital step of which the objective is to label the positions and classes of object spots in the diseased images. For this stage, an algorithm that provides a frame selection function is developed in Python. With this algorithm and knowledge that is provided by experts in the field of agriculture, the diseased areas of an image can be selected and labeled with the corresponding classes. All the disease images in the dataset have been annotated. After the annotation step, the program will generate XML files for each annotated image that contain information such as the coordinate values of each lesion's bounding boxes and the classes of the diseases.

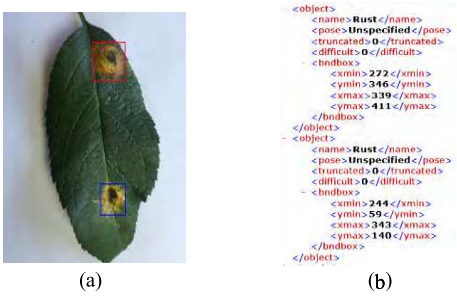

FIGURE 3. Annotation of the apple leaf disease dataset. (a) Annotated image. (b) XML document.

Considering a rust-infected leaf as an example, Figure 3(a) shows an annotated image. The red and blue boxes indicate the infected areas of the diseased apple leaf. Figure 3(b) shows the corresponding description of the image, which is in the form of an XML document.

3) DATA AUGMENTATION

The overfitting problem in the training stage of CNNs can be overcome via data augmentation. The overfitting problem occurs when random noise or errors, rather than the underlying relationship, are described [27]. With more images after expansion via data augmentation techniques, the model can learn as many irrelevant patterns as possible during the training process, thereby avoiding overfitting and realizing higher performance.

In this step, several techniques are used for data augmentation operations, including rotation transformations, horizontal and vertical flips, and intensity disturbance, which include disturbances of brightness, sharpness and contrast. A Gaussian noise processing operation is also applied. Via the above operations, 12 new diseased images are generated from each image, as shown in Figure 4.

III. DETECTION MODEL OF APPLE LEAF DISEASES

Inspired by the SSD, a new real-time detection model, namely, INAR-SSD, is proposed. It consists of two parts,

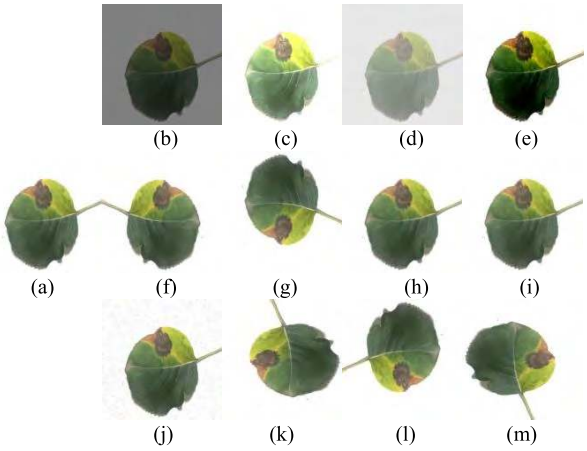

FIGURE 4. Data augmentation of apple leaf disease images: (a) Original image; (b) Low brightness; (c) High brightness; (d) Low contrast; (e) High contrast; (f) Vertical flip; (g) Horizontal flip; (h) Low sharpness; (i) High sharpness; (j) Gaussian noise; (k) 90° rotation; (l) 180° rotation; and (m) 270° rotation.

namely, a basic pre-network and a feature extraction and fusion structure, as illustrated in Figure 5. To increase network's adaptability to various scales of apple leaf disease spots, conv4_1 and conv4_2 of VGGNet [25] are replaced with two GoogLeNet Inception modules. Via this approach, the capability of multi-scale feature extraction can be improved. The feature extraction and fusion structure is designed by applying the Rainbow concatenation method to improve the feature fusion performance. Pooling and deconvolution are performed simultaneously to create feature maps among layers so that when the detection is performed, all the cases are considered, regardless of whether the size of the object is appropriate for the specified scale or not. This improved SSD model implements multi-angle feature fusion by utilizing the Inception module to extract features of various sizes and Rainbow concatenation to enhance contextual connections among layers, with the objective of improving the detection performance for small apple leaf disease spots.

A. SINGLE-SHOT MULTI-BOX DETECTOR

SSD [24] is a one-stage object detection method that can predict the types of objects and the coordinates of the corresponding bounding boxes directly, without generating region proposals. The SSD model combines several feature maps with various resolutions to process objects of various sizes. The detection speed of SSD is much faster than that of Faster R-CNN [28], [29], while the detection accuracies of the two methods are approximately the same. Thus, the SSD algorithm is used as the basic object detection algorithm and improved with multi-angle feature fusion.

B. STRUCTURE OF THE INCEPTION MODULE

The most straightforward way to improve the feature extraction capability of deep neural networks is to increase the depth or the width of the model. However, this may result in two problems: One problem is that a deeper or wider model typically has more parameters, thereby making the enlarged network prone to overfitting. The other problem is a substantial increase in computing resource consumption. To overcome these problems and extract features more effectively, the Inception module utilizes parallel layers of various convolution kernel sizes and concatenates their outputs at the end of the module to realize the integration of features and enhance the adaptability of the network to various scales [30]. Inception has been improved by replacing a single 5x5 convolution layer with two cascaded 3×3 convolution layers [31], which not only maintains the range of perceptive fields but also reduces the number of parameters. As illustrated in Figure 6, the Inception module consists of parallel 1×1 convolution layers, 3×3 convolution layers and two cascaded 3×3 convolution layers that are beside a max-pooling layer, which can abstract a vast variety of features in parallel. In addition, 1×1 convolution layers are inserted before or after the parallel convolution layers to reduce the number of weights and the feature map dimensions.

Considering the above features of Inception, two Inception modules, as illustrated in Figure 6, are added to VGG-16 to improve the multi-scale feature extraction ability of the new network, namely, VGG-INCEP, to solve the problem of detecting disease spots of various sizes on the same leaf.

C. VGG-INCEP NETWORK MODEL

Since VGGNet [25] is often used for migration learning, the model is highly portable. In addition, according to the results that are listed in Table 4, among conventional convolution neural networks, VGGNet has a higher accuracy in identifying apple leaf diseases. Therefore, VGGNet is selected as the basic pre-network model.

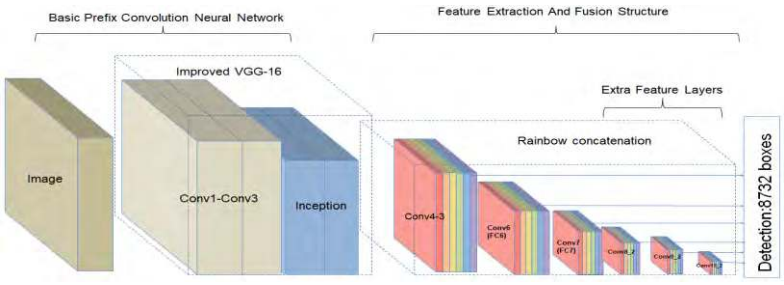

FIGURE 5. Overall structure of INAR-SSD.

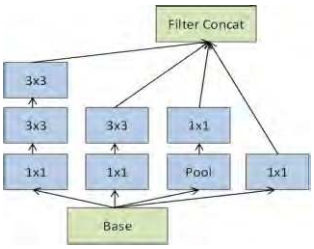

FIGURE 6. Inception module.

TABLE 1. Related parameters of the VGG-INCEP model.

Name	Type	Kernel Size/Stride	Output Size
Conv1_1	Convolution	3x3/1	224x224x64
Conv1_2	Convolution	3x3/1	224x224x64
Pool1	Pool/Max	2x2/2	112x112x64
Conv2_1	Convolution	3x3/1	112x112x128
Conv2_2	Convolution	3x3/1	112x112x128
Pool2	Pool/Max	2x2/2	56x56x128
Conv3_1	Convolution	3x3/1	56x56x256
Conv3_2	Convolution	3x3/1	56x56x256
Conv3_3	Convolution	3x3/1	56x56x256
Pool3	Pool/Max	2x2/2	28x28x256
Inception_stem1	Inception Module	——	28x28x576
Inception_stem1	Inception Module	——	28x28x576
Conv4_3	Convolution	3x3/1	28x28x512
Pool4	Pool/Max	2x2/2	14x14x512
Conv5_1	Convolution	3x3/1	14x14x512
Conv5_2	Convolution	3x3/1	14x14x512
Conv5_3	Convolution	3x3/1	14x14x512
Pool5	Pool/Max	2x2/2	7x7x512
Conv6	Convolution	7x7/1	1x1x4096
Conv7	Convolution	1x1/1	1x1x4096
Conv8	Convolution	1x1/1	1x1x5
Softmax	Softmax	——	5

Detailed parameters of the adjusted VGGNet, which is named the VGG-INCEP network, are listed in Table 1. The first few layers of a convolutional neural network typically extract the color and corner features [32], [33] and it is of little value to utilize Inception to extract these features. Hence, the Conv1_1 to Pool3 layers of the VGGNet are preserved and subsequent layers Conv4_1 and Conv4_2 of VGGNet are replaced with two Inception modules, as discussed above, to enhance the multi-scale feature extraction ability of the network. Then, layers Conv4_3 to Pool5 are set behind the Inception modules without modification. For Conv6 to Conv8, to overcome the input size limitation of the network, the full connection layers of VGGNet are replaced with 1x1 convolution layers. The final layer is a five-way Softmax layer.

D. RAINBOW CONCATENATION

The original SSD algorithm has two main drawbacks: One is that the same object can be detected in multiple scales of feature maps because each layer in the feature pyramid is used independently as an input to the classifier network. The other is that the performance of SSD in detecting small objects is limited. Thus, an algorithm that is dedicated to solving these two problems, namely, R-SSD, is proposed, which applies Rainbow concatenation to the SSD algorithm.

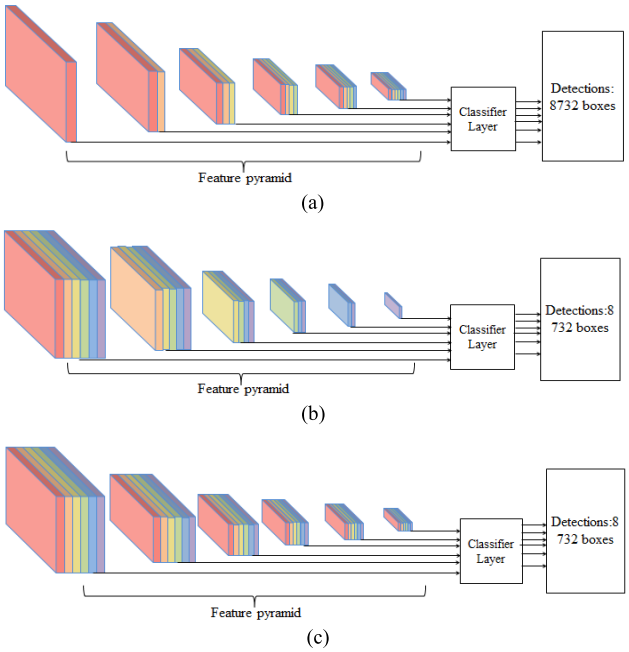

FIGURE 7. Three types of feature concatenation. (a) Pooling. (b) Deconvolution. (c) Both pooling and deconvolution (Rainbow concatenation).

The methodology of Rainbow concatenation, which is implemented in R-SSD [26], is applied to further improve the detection accuracy for small objects that correspond to apple leaf diseases. Figure 7 presents three approaches to increasing the number of feature maps to take advantage of the relationships among the layers in the feature pyramid. In Figure 7(a), feature maps in the lower layers are concatenated to those of the upper layers via pooling, while in Figure 7(b), feature maps in the upper layers are concatenated to those of the lower layers via deconvolution. However, using pooling or deconvolution separately only allows the contextual information to flow in one direction. Therefore, in R-SSD, these two methods are both applied to produce an explicit relationship of feature maps among layers. By using Rainbow concatenation, the detection precision of small objects is substantially improved.

IV. EXPERIMENTAL EVALUATION

In this section, the experimental setup is introduced. Then, details of the experimental platform and benchmarks are provided. Finally, the experimental results are analyzed and discussed.

A. EXPERIMENTAL SETUP

This experiment was performed on an Ubuntu server with an Intel ® Xeon(R) CPU E5-2650 v3 @ 2.30 GHz ×40 that was accelerated by an NVIDIA GTX1080Ti GPU. NVIDIA GTX1080Ti has 3,584 CUDA cores and 11 GB memory. The core frequency is up to 1480 MHz and the floating-point performance is 10.5 TFLOPS. The CNN-based model was implemented in the Caffe deep learning framework. Additional configuration parameters are listed in Table 2.

TABLE 2. Hardware and software environment.

Configuration Item	Value
CPU	Intel® Xeon(R) CPU E5-2650 v3
GPU	NVIDIA GTX1080Ti 11 GB
Memory	128 GB
Hard disk	2 TB
Operating system	Ubuntu 16.04.2 LTS(64-bit)

TABLE 3. Apple leaf disease dataset.

Disease	Training/Testing Images	Total Number
Alternaria leaf spot	4121/1222	5343
Brown spot	4316/1339	5655
Mosaic	3770/1105	4875
Grey spot	3328/1482	4810
Rust	4238/1456	5694
Total	19773/6604	26377

B. DATASET

The proposed model has been evaluated on the collected ALDD, which contains images of 5 common apple leaf diseases that were captured in the laboratory and in the field. By applying an image processing technique, a total of 26,377 disease images were generated. To perform the experiment, 75% of the dataset is used for training and the other 25% for testing; the ratio of the size of the training dataset to that of the validation dataset is 4:1. Table 3 lists the numbers of training sets and testing sets for the apple leaf diseases.

C. EXPERIMENTAL RESULTS AND ANALYSES

1) COMPARISON OF PRE-NETWORK RECOGNITION ACCURACY

Object detection algorithms such as SSD, DSSD and R-SSD can be regarded as consisting of two parts: The first part is the pre-network model, which is used as a basic feature extractor. The other is an auxiliary structure that utilizes multi-scale feature maps for detection.

In this section, several deep convolution networks – AlexNet [34], GoogLeNet [30], InceptionV3 [31], ResNet-101, ResNet-50, ResNet-34, ResNet-18 [35] and VGGNet-16 [25] – are trained and tested to compare the recognition performances of traditional networks with that of our proposed VGG-INCEP on ALDD. During training, the stochastic gradient descent (SGD) algorithm is applied to learn the set of weights and biases of the neural network that minimize the loss function. The SGD algorithm randomly selects a small number of training sets, which is referred to as the batch size. The batch size is set to 32 and the learning rate is set to 0.001, which is small but leads to more precise results. To determine how fast the SGD algorithm converges to the optimum point, the momentum, which serves as an additional factor, is set to 0.9.

As shown in Figure 8, the accuracy curve is plotted with the number of training iterations on the X-axis and the corresponding training accuracy on the Y-axis. In this comparison experiment, the test accuracies of various pre-networks are listed in Table 4 and the accuracy curves are

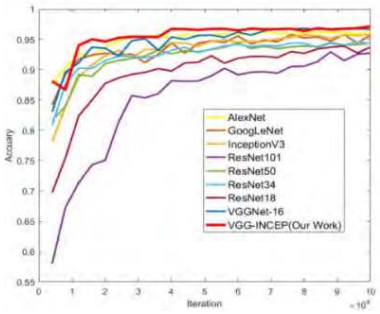

FIGURE 8. Comparison in terms of convergence speed and training accuracy.

TABLE 4. Test accuracies of nine pre-networks.

Pre-network model	Input size	Recognition accuracy (%)
AlexNet	227	95.78
GoogLeNet	224	94.85
InceptionV3	232	95.49
ResNet-101	224	91.16
ResNet-50	224	92.43
ResNet-34	224	93.17
ResNet-18	224	93.64
VGGNet-16	224	96.10
VGG-INCEP(Our work)	224	**97.14**

plotted in Figure 8. AlexNet, VGGNet-16, GoogLeNet, and InceprionV3 outperform ResNet. Meanwhile, on the ALDD, it is not the case that the more layers of the convolutional neural network, the higher the recognition accuracy. In contrast with ResNet-34, ResNet-50 and ResNet-101 [35] contain 50 and 101 layers, respectively, but both networks have lower convergence speed and recognition accuracy when applied to ALDD. In addition, by combining VGGNet-16 and InceptionV3, the proposed model, namely, VGG-INCEP, realizes the top performances in terms of both the final accuracy and the convergence speed in this comparative experiment.

2) CONFUSION MATRIX

Classifiers can be confused when faced with multiple classes of similar shape. Infected apple leaf images at different stages or against different backgrounds may also lead to high complexity of the patterns that are displayed in the same class, which results in lower performance. A confusion matrix can be used to visually estimate the classification accuracy of a model.

Figure 9 shows the confusion matrix of the final test results. The deeper the color in the visualization results, the higher the prediction accuracy of the model in the corresponding class. All correct predictions are on the diagonal and all incorrect predictions are off the diagonal; hence, the classes have confused the detecting system can be conveniently and intuitively identified.

Based on these results, the performance of the classifier can be visually evaluated. These results can also enable us to study how to better avoid confusion among classes to improve the performance of the model. According to the analysis of

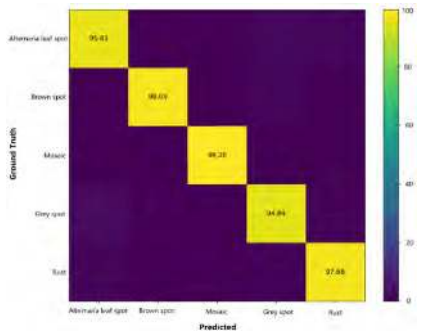

FIGURE 9. Confusion matrix of the ALDD recognition results.

the above five diseases, the features of Mosaic and Brown spot diseases differ substantially from those of other diseases and reach recognition rates of 99.26% and 98.09%, respectively. According to the confusion matrix, compared with other classes, the detection is more prone to confusion in distinguishing Alternaria leaf spot and Grey spot: 27 Alternaria leaf spot images, out of a total of 1,335 images in the testing set, were incorrectly identified as Grey spot. This is due to the similarity in geometric features between the two diseases. Nevertheless, other classes are well differentiated. The confusion matrix provides an explanation for the low recognition accuracies on several classes in our experiment.

3) RESULT COMPARISON OF VARIOUS DETECTION ALGORITHMS

To compare the performances of various detection algorithms, INAR-SSD, Faster R-CNN, SSD and other object detection algorithms are applied to detect apple leaf diseases.

In the evaluation of the object detection algorithms, the mean average accuracy (mAP) is the main evaluation indicator in this paper [36]. With the same input size of 512×512, our proposed model reaches 78.80% mAP and outperforms SSD-VGGNet on all classes, with a higher total accuracy by 2.98%. At the same time, our model has the highest accuracy in the detection of two types of diseases: Alternaria leaf spot and Grey spot.

During the experiment, R-SSD and DSSD [37] are also applied to evaluate the recognition performances of other improved versions of SSD on ALDD. The results demonstrate that there have been enhancements in RSSD. Compared to SSD-VGGNet, with input images of the same size, the two versions of RSSD-VGGNet improved the total accuracy by 1.74% and 1.72%, respectively. Meanwhile, the performance of DSSD is barely satisfactory in terms of total accuracy. However, DSSD has the highest test accuracy for Brown spot and Rust, while it has almost the lowest test accuracy for all other classes.

To determine whether using deeper networks also improves our performance, two base networks, namely, VGGNet [25] and ResNet-101 [35], are used as feature extractors for SSD. The experimental results demonstrate that ResNet-101 does not result in an improvement; it yields similar results to the pre-network experiments. Hence, the deep ResNet network is not suitable for our dataset. The recognition accuracies of SSD300 and SSD512 decreased by 2.07% and 1.00%, respectively. Using the same feature extractor, namely, VGGNet, the total accuracy of Faster R-CNN is close to that of SSD and that of the latter is slightly higher. Furthermore, SSD performs better at distinguishing between Alternaria leaf spot and Grey spot, while on Mosaic it underperforms Faster R-CNN in terms of recognition accuracy.

In the experiment, Alternaria leaf spot, Grey spot and Mosaic are regarded as the most complex classes. This is due to their large within-class differences: colors can be light or dark and spots can be large or small for all three diseases. Moreover, the high similarity between Alternaria leaf spot and Grey spot renders them more difficult to distinguish. Meanwhile, the Rust's recognition accuracy for all models was stable at approximately 90% because there is little variation among the lesions' patterns from rust-infected leaves and the shape of the lesions differs substantially from those of other classes and, hence, can be easily distinguished even by visual observation.

4) DATA AUGMENTATION COMPARISON EXPERIMENTS

To prevent overfitting, in this paper, various methods have been utilized. First, the diseased apple leaves were captured in various environments and under various weather conditions. Most diseased apple images with complex backgrounds were collected in the apple orchard, while a few other diseased images with uniform backgrounds were captured in a lab environment. By selecting various shooting backgrounds, the generalization of the proposed model can be ensured, which reduces the occurrence of overfitting. Second, various digital image processing technologies such as rotation transformations, mirror symmetry and intensity disturbance were applied to the natural training images to simulate the real acquisition environment and increase the diversity and quantity of the apple leaf training images, which can prevent overfitting and improve the generalization performance of the proposed model during the training process.

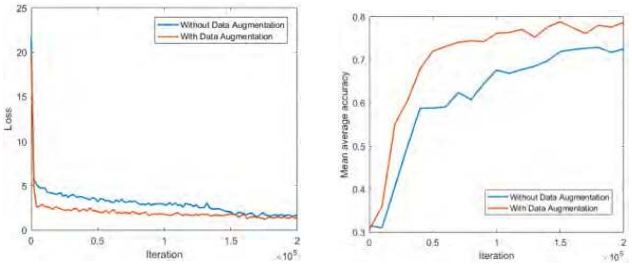

(a) (b)

FIGURE 10. Influence of the expanded dataset. (a) Training loss. (b) Test accuracy.

Data augmentation is a satisfactory option when the training dataset is insufficient or to prevent overfitting to make the model more robust. This paper performed two sets of experiments to estimate the performance of the dataset for the proposed model, which was trained separately before and after the expansion of the dataset. As shown in Figure 10,

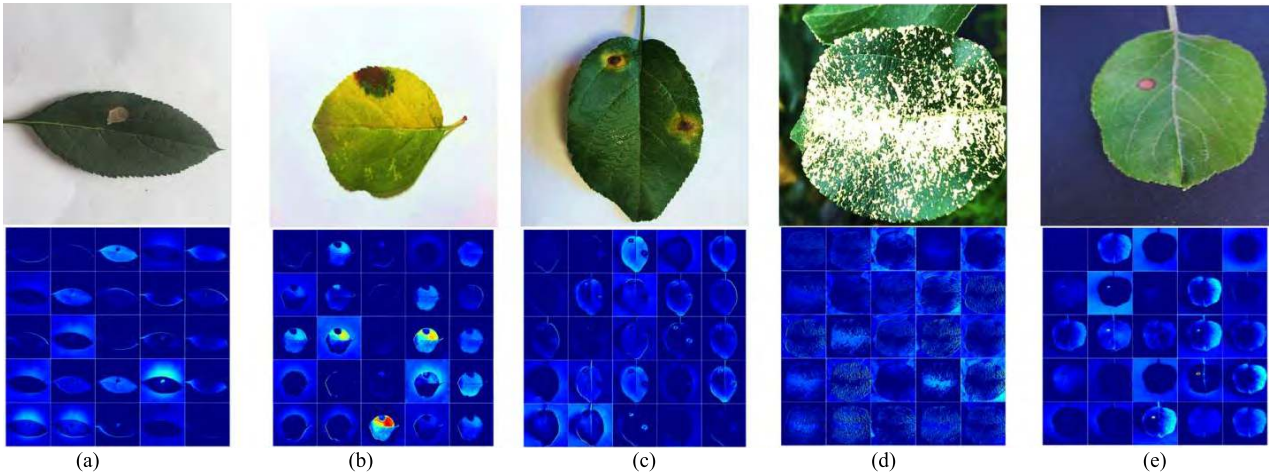

FIGURE 11. Activation visualization results. (a) Grey spot. (b) Brown spot. (c) Rust. (d) Mosaic. (e) Alternaria leaf spot.

TABLE 5. Test results for various detection models.

Method	Faster R-CNN		SSD		SSD		DSSD	R-SSD	R-SSD	IAR-SSD
Feature Extractor / Classes	ZFNet	VGGNet	VGGNet	ResNet-101	VGGNet	ResNet-101	ResNet-101	VGGNet	VGGNet	VGG-INCEP
Input			300	300	512	512	321	300	512	512
Alternaria leaf spot	58.82	63.27	69.96	67.59	73.01	68.03	65.59	70.29	74.41	**75.56**
Brown spot	68.12	76.33	76.45	75.21	75.85	77.69	**80.54**	76.50	78.19	79.70
Mosaic	**79.20**	78.91	71.23	71.02	72.50	78.08	71.44	74.46	75.78	76.50
Grey spot	48.00	59.72	63.28	57.29	67.19	60.29	57.56	68.62	68.77	**70.63**
Rust	90.34	90.67	90.72	90.20	90.53	90.03	**93.46**	90.48	90.55	91.59
mAP	68.90	73.78	74.33	72.26	75.82	74.82	73.12	76.07	77.54	**78.80**

without data augmentation, the training process has high loss and low accuracy and finally reaches 71.89% mAP. However, the proposed model with data augmentation realizes 78.80% mAP, which corresponds to a detection precision improvement of 6.91% over the dataset without data augmentation.

5) FEATURE VISUALIZATION PROCESS

The weak explanatory ability of the CNN makes it a ''black box'' model. Other factors, such as its multi-layer hidden structure and massive number of parameters, also defy understanding. To determine how CNNs learn features for distinguishing among classes, visualization techniques are used to reveal CNN feature maps. Through this experiment, the differences among the feature maps that are extracted from various diseased apple images can be better understood.

According to the visualization results that are shown in Figure 11, all the disease spots are clearly separated from the background images; hence, the proposed model has excellent discrimination performance for apple leaf diseases. The visualization result for Mosaic that is shown in Figure 11(d) has substantial differences with those of other diseases because its lesion diffuses throughout the whole leaves. Brown spot is typically large and the boundaries are not clear, as shown in Figure 11(b). For Rust, the spots are separated into two laps in Figure 11(c) and the inner lap is the aecidium. Moreover, in Figure 11(a) and Figure 11(e), though Grey spot and Alternaria leaf spot are similar, they can still be classified according to their differences. Alternaria leaf spot is rounder and smaller than Grey spot. In this experiment, the activation visualization results for various apple leaf diseases demonstrate the strong performance of the proposed model in detecting diseases and clarify how CNNs learn features for distinguishing among classes.

6) ACCURACY VS. SPEED

The detection speed is another important indicator of the object detection algorithm, which has a crucial effect on real-time detection. In our experiments, Faster R-CNN, SSD, DSSD, RSSD and our proposed model have been evaluated in terms of detection speed. The detailed data are listed in Table 6. Faster R-CNN has high precision in the two-stage detection algorithm. However, the running speed of Faster R-CNN is slow, thereby weakening the real-time detection performance. The conventional SSD is one of the most advanced object detection algorithms at present in terms of both accuracy and speed. For SSD300 or SSD512 with VGGNet as the basic pre-network, the testing results are 74.33% mAP with 47.35 FPS and 75.82% mAP with 28.95 FPS, respectively. For R-SSD, although its speed decreased to 37.88 FPS and 23.01 FPS, it realized 1.74% and 1.72% accuracy gains compared to conventional SSD.

TABLE 6. Accuracy vs speed for various models.

Method	Faster R-CNN		SSD		SSD		DSSD	R-SSD	R-SSD	IAR-SSD
Classes \ Feature Extractor	ZFNet	VGGNet	VGGNet	ResNet-101	VGGNet	ResNet-101	ResNet-101	VGGNet	VGGNet	VGG-INCEP
Input			300	300	512	512	321	300	512	512
mAP	68.90	73.78	74.33	72.26	75.82	74.82	73.12	76.07	77.54	78.80
FPS	14.91	7.79	47.35	28.26	28.95	13.41	9.62	37.88	23.01	23.13

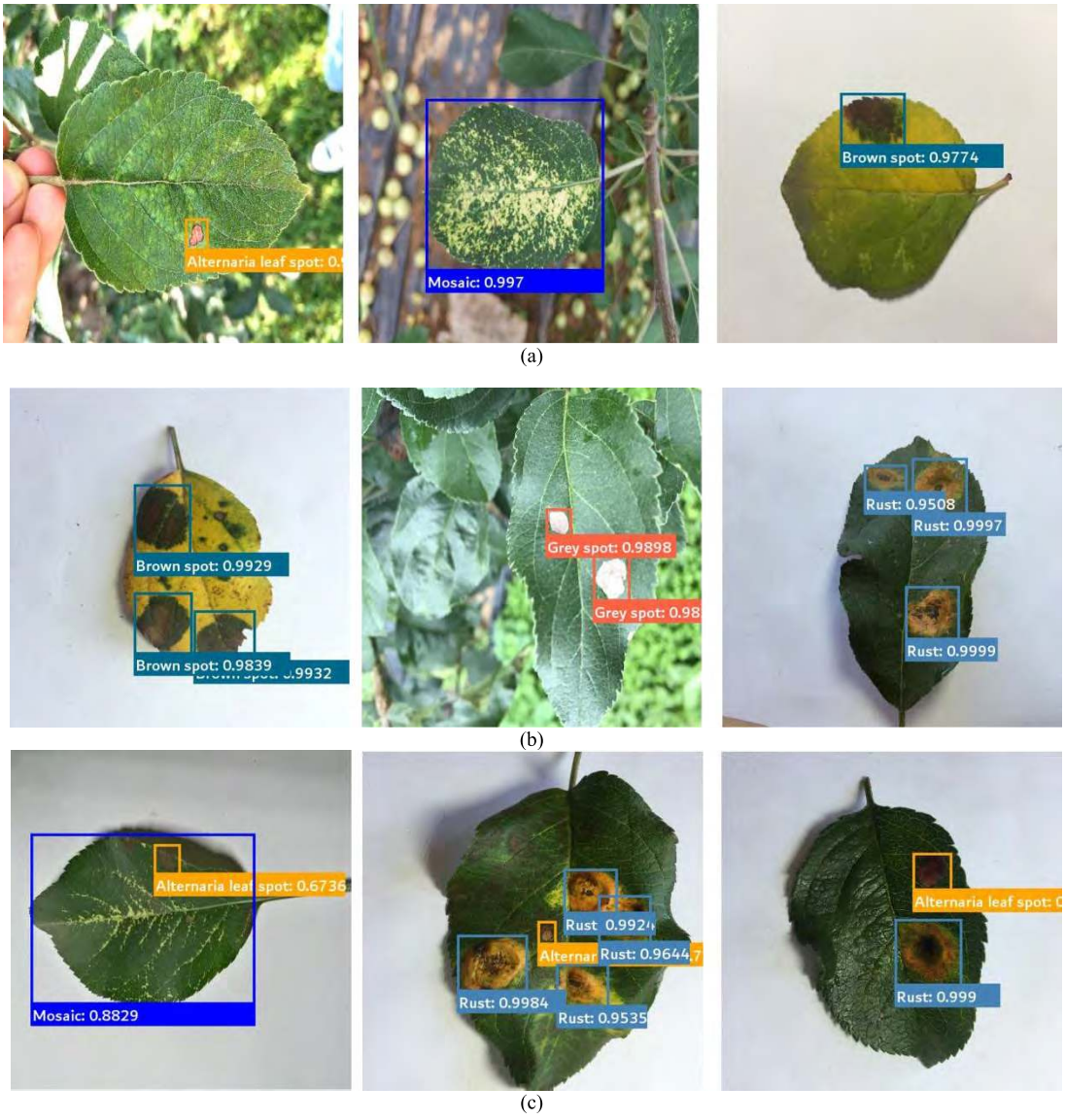

FIGURE 12. Types of detection results. (a) Single object of a single class. (b) Multiple objects of a single class. (c) Multiple objects of multiple classes.

In the experiments, INAR-SSD realizes 78.80% mAP and 23.13 FPS, which corresponds to 2.98% mAP improvement, although with a slower speed compared to conventional SSD. Compared to R-SSD, our proposed algorithm realizes higher accuracy and faster detection speed.

7) DETECTION VISUALIZATION AND FAILURE ANALYSIS

Images of detection results are shown in Figure 12. The proposed method can not only detect a single object of single class but also multiple objects of a single class and multiple objects of multiple classes, which demonstrates its formidable detection performance.

Although our method exhibits excellent performance in this case, detection failures are observed. Figure 13(a) shows an example of an erroneous identification of Alternaria leaf spot and Grey spot. According to the confusion matrix, these two diseases are easily confused, which leads to a low recognition accuracy for both of them. The accuracy reduction

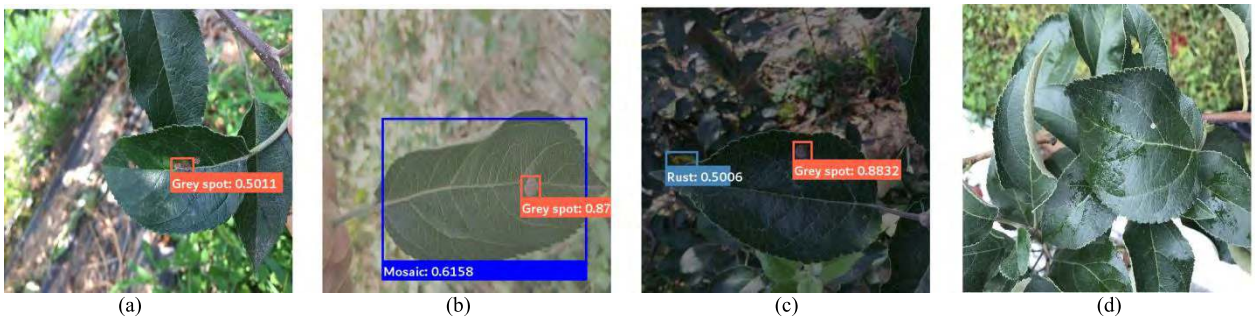

FIGURE 13. Incorrect detection: (a) Identifying an Alternaria leaf spot as a Grey spot; (b) Identifying background as Mosaic; (c) Identifying background as Rust; (d) Identifying nothing when there is a Grey spot object.

is due to the similar characteristics of the diseases. The recognition accuracy is also affected by environmental factors such as complex background, lighting, and blur. As shown in Figure 13(b), due to the dark background and overly clear leaf meridians, the background is mistaken for Mosaic by the detection algorithm. Moreover, as a result of the bright orange color of Rust, a piece of the background is recognized as Rust in Figure 13(c). In addition, the lesion's small size is one of the factors that leads to an increase in detection failures. If the leaf or the diseased area occupies only a tiny proportion of the image, the extraction and detection of the feature will be difficult. As shown in Figure 13(d), the detection algorithm cannot identify an extremely small object as a Grey spot.

V. RELATED WORK

Plant diseases are a major threat to plant growth and crop yield and many researchers have expended substantial efforts on detecting plant diseases. Traditionally, visual examination by experts has been carried out to diagnose plant diseases and biological examination is the second option, if necessary. In recent years, through the development of computer technology, machine learning has been widely utilized to train and detect plant diseases and is a satisfactory alternative for the detection of plant diseases.

In [5], Zhang *et al.* proposed an apple leaf disease recognition method that is based on image processing techniques and pattern recognition methods. In the experiment, on an image database of diseased apple leaves that contained 90 disease images (including classes: healthy apple leaf, powdery mildew leaf, mosaic leaf and rust leaf), this approach realized a recognition accuracy of more than 90%. In [8], Bashish *et al.* provided a fast, automatic, cheap and accurate image-based solution for the identification of leaf diseases. The proposed solution is composed of four main phases: a color transformation structure, image segmentation via the K-means clustering technique, calculation of the texture features and, finally, a pre-trained neural network for transmitting the extracted features. The experimental results demonstrated that the scheme could successfully detect and classify diseases with an accuracy rate of approximately 93%. In [38], Waghmare *et al.* proposed a method for identifying plant diseases via leaf texture analysis and pattern recognition. The system took a plant image as an input and the segmented leaf image was analyzed by using a high-pass filter to detect the diseased part of the leaf. In the experimental part, common downy mildew, black rot and other diseases of grape plants were classified systematically and the accuracy rate was 96.6%. In [6], Arivazhagan *et al.* proposed an algorithm for classifying plant leaf diseases according to texture features. In the processing scheme, images were subjected to a color conversion structure and a segmentation mechanism. Finally, the extracted features were passed through a support vector machine classifier. The algorithm effectively detected and classified the examined diseases with an accuracy of 94%. However, traditional machine learning approaches require complicated image preprocessing, feature extraction and classification steps [39], [40]; it is easier to realize higher accuracy by using a deep learning approach that is based on convolution neural networks.

In recent years, several researchers have studied plant disease recognition based on deep learning approaches. In [18], Mohanty *et al.* trained a deep convolutional neural network to identify 14 crop species and 26 diseases using a public dataset of 54,306 images. The trained model realized an accuracy of 99.35%. When tested on a set of images from online sources instead of the images that were used for training, the model still realized an accuracy of 31.4%. In [41], Ferentinos trained multiple CNN architectures, such as AlexNet, VGG and GoogLeNet, using an open database that contained 58 combinations of plants or diseases. The experimental results demonstrated that the most successful model architecture was the VGG convolution neural network, which realized a success rate of 99.53%. In [22], Liu *et al.* designed a new architecture of deep convolutional neural networks that was based on AlexNet for detecting apple leaf diseases. On a dataset that contained Mosaic, Rust, Brown spot, and Alternaria leaf spot, a recognition accuracy of 97.62% was realized. In [42], Ramcharan *et al.* applied transfer learning to train CNNs to identify three diseases and two types of pest damage and the best model realized an overall accuracy of 93%. The main drawback of these studies is the use of image recognition technology that can only identify a single object at a time. Moreover, the requirements for real-time monitoring of multiple diseases in a complex context

have been ignored, which are of significance for practical applications.

Therefore, researchers have begun to study the application of object detection to plant disease detection. In [43], Johannes *et al.* proposed a novel image processing algorithm that is based on candidate hot-spot detection and detected three European endemic wheat diseases– septoria, rust and tan spot. The results revealed area under the receiver operating characteristic–ROC–curve (AuC) metrics of higher than 0.80. In [19], Fuentes *et al.* proposed a deep learning method for detecting tomato pests and diseases. A comparative experiment was conducted in which three networks, namely, faster R-CNN, SSD and R-FCN, were used to detect 9 tomato diseases. The experimental results demonstrate that this method can effectively detect tomato diseases and can handle complex backgrounds. In [20], Lu *et al.* proposed an on-site automatic diagnosis system for wheat diseases that is based on a weak supervised deep learning framework. They also collected a new image dataset for wheat diseases, namely, WDD2017, which was used to evaluate the performance of the system. Using two architectures, namely, VGG-FCN-VD16 and VGG-FCN-S, the average recognition accuracy reached 97.95% and 95.12%, respectively, and the recognition accuracy was higher than those of the traditional CNN architectures.

According to these studies, convolution neural networks have been used extensively in the field of crop disease identification and satisfactory results have been obtained. However, object detection has not been applied to the real-time monitoring of apple leaf diseases, which is of high practical value for agricultural applications. Another shortcoming is that the application-oriented object detection algorithm is seldom improved. Therefore, in our work, an object detection model for the detection of apple leaf diseases is proposed.

VI. CONCLUSION

This paper has proposed a real-time detection approach that is based on improved convolutional neural networks for apple leaf diseases. The deep-learning-based approach can automatically extract the discriminative features of the diseased apple images and detect the five common types of apple leaf diseases with high accuracy in real time. In this study, to ensure satisfactory generalization performance of the proposed model and a sufficient apple disease image dataset, a total of 26,377 images with uniform and complex backgrounds were collected in the laboratory and in a real apple field and generated via data augmentation technology. Furthermore, the new deep convolution neural network model, namely, INAR-SSD, was designed by introducing the GoogLeNet Inception module and integrating the Rainbow concatenation to enhance the multi-scale disease object detection and small diseased object detection performances.

The new deep-learning-based approach was implemented in the Caffe framework on the GPU platform. Using a dataset of 26,377 images of diseased leaves, the proposed model, namely, INAR-SSD, was trained to detect apple leaf diseases. The comprehensive detection performance reaches 78.80% mAP. Meanwhile, the detection speed of the model reaches 23.13 FPS. Hence, the proposed model is fully capable of real-time detection of apple leaf diseases. The results demonstrate that the proposed INAR-SSD model can detect the five common types of apple leaf diseases with high accuracy in real time and provides a feasible solution for the real-time detection of apple leaf diseases.

REFERENCES

[1] M. Dutot, L. M. Nelson, and R. C. Tyson, "Predicting the spread of postharvest disease in stored fruit, with application to apples," *Postharvest Biol. Technol.*, vol. 85, pp. 45–56, Nov. 2013.

[2] A.-K. Mahlein *et al.*, "Development of spectral indices for detecting and identifying plant diseases," *Remote Sens. Environ.*, vol. 128, pp. 21–30, Jan. 2013.

[3] L. Yuan, Y. Huang, R. W. Loraamm, C. Nie, J. Wang, and J. Zhang, "Spectral analysis of winter wheat leaves for detection and differentiation of diseases and insects," *Field Crops Res.*, vol. 156, no. 2, pp. 199–207, Feb. 2014.

[4] F. Qin, D. Liu, B. Sun, L. Ruan, Z. Ma, and H. Wang, "Identification of alfalfa leaf diseases using image recognition technology," *PLoS ONE*, vol. 11, no. 12, 2016, Art. no. e0168274.

[5] Z. Chuanlei, Z. Shanwen, Y. Jucheng, S. Yancui, and C. Jia, "Apple leaf disease identification using genetic algorithm and correlation based feature selection method," *Int. J. Agricult. Biol. Eng.*, vol. 10, no. 2, pp. 74–83, 2017.

[6] S. Arivazhagan, R. N. Shebiah, S. Ananthi, and S. V. Varthini, "Detection of unhealthy region of plant leaves and classification of plant leaf diseases using texture features," *Agricult. Eng. Int., CIGR J.*, vol. 15, no. 1, pp. 211–217, 2013.

[7] S. B. Dhaygude and N. P. Kumbhar, "Agricultural plant leaf disease detection using image processing," *Int. J. Adv. Res. Elect., Electron. Instrum. Eng.*, vol. 2, no. 1, pp. 599–602, 2013.

[8] D. Al Bashish, M. Braik, and S. Bani-Ahmad, "Detection and classification of leaf diseases using k-means-based segmentation and neural-networks-based classification," *Inf. Technol. J.*, vol. 10, no. 2, pp. 267–275, 2011.

[9] P. Rajan, B. Radhakrishnan, and L. P. Suresh, "Detection and classification of pests from crop images using support vector machine," in *Proc. Int. Conf. Emerg. Technol. Trends*, Oct. 2017, pp. 1–6.

[10] T. Rumpf, A.-K. Mahlein, U. Steiner, E.-C. Oerke, H.-W. Dehne, and L. Plümer, "Early detection and classification of plant diseases with support vector machines based on hyperspectral reflectance," *Comput. Electron. Agricult.*, vol. 74, no. 1, pp. 91–99, 2010.

[11] M. Islam, A. Dinh, K. Wahid, and P. Bhowmik, "Detection of potato diseases using image segmentation and multiclass support vector machine," in *Proc. IEEE 30th Can. Conf. Elect. Comput. Eng.*, Apr./May 2017, pp. 1–4.

[12] C. Wu, C. Luo, N. Xiong, W. Zhang, and T. Kim, "A greedy deep learning method for medical disease analysis," *IEEE Access*, vol. 6, pp. 20021–20030, 2018.

[13] H. Lu, Y. Li, M. Chen, H. Kim, and S. Serikawa, "Brain intelligence: Go beyond artificial intelligence," *Mobile Netw. Appl.*, vol. 23, no. 2, pp. 368–375, Apr. 2018.

[14] J. Li, N. Wang, Z.-H. Wang, H. Li, C.-C. Chang, and H. Wang, "New secret sharing scheme based on faster R-CNNs image retrieval," *IEEE Access*, vol. 6, pp. 49348–49357, 2018.

[15] A. Caglayan and A. B. Can, "Volumetric object recognition using 3-D CNNs on depth data," *IEEE Access*, vol. 6, pp. 20058–20066, 2018.

[16] H. Lu, Y. Li, T. Uemura, H. Kim, and S. Serikawa, "Low illumination underwater light field images reconstruction using deep convolutional neural networks," *Future Gener. Comput. Syst.*, vol. 82, pp. 142–148, May 2018.

[17] C. DeChant *et al.*, "Automated identification of northern leaf blight-infected maize plants from field imagery using deep learning," *Phytopathology*, vol. 107, no. 11, pp. 1426–1432, 2017.

[18] S. P. Mohanty, D. P. Hughes, and M. Salathé, "Using deep learning for image-based plant disease detection," *Frontiers Plant Sci.*, vol. 7, p. 1419, Sep. 2016.

[19] A. Fuentes, S. Yoon, S. C. Kim, and D. S. Park, "A robust deep-learning-based detector for real-time tomato plant diseases and pests recognition," *Sensors*, vol. 17, no. 9, p. 2022, 2017.
[20] J. Lu, J. Hu, G. Zhao, F. Mei, and C. Zhang, "An in-field automatic wheat disease diagnosis system," *Comput. Electron. Agricult.*, vol. 142, pp. 369–379, Nov. 2017.
[21] Y. Lu, S. Yi, N. Zeng, Y. Liu, and Y. Zhang, "Identification of Rice diseases using deep convolutional neural networks," *Neurocomputing*, vol. 267, pp. 378–384, Dec. 2017.
[22] B. Liu, Y. Zhang, D. J. He, and Y. Li, "Identification of apple leaf diseases based on deep convolutional neural networks," *Symmetry*, vol. 10, no. 1, pp. 1–16, 2017.
[23] X. Zhang, Y. Qiao, F. Meng, C. Fan, and M. Zhang, "Identification of maize leaf diseases using improved deep convolutional neural networks," *IEEE Access*, vol. 6, pp. 30370–30377, 2018.
[24] W. Liu *et al.*, "SSD: Single shot multibox detector," in *Proc. Eur. Conf. Comput. Vis.*, 2016, pp. 21–37.
[25] K. Simonyan and A. Zisserman. (2014). "Very deep convolutional networks for large-scale image recognition." [Online]. Available: https://arxiv.org/abs/1409.1556
[26] J. Jeong, H. Park, and N. Kwak. (2017). "Enhancement of SSD by concatenating feature maps for object detection." [Online]. Available: https://arxiv.org/abs/1705.09587
[27] S. Heisel and T. Kova ević, "Variable selection and training set design for particle classification using a linear and a non-linear classifier," *Chem. Eng. Sci.*, vol. 173, pp. 131–144, Dec. 2017.
[28] S. Ren, K. He, R. Girshick, and J. Sun, "Faster R-CNN: Towards real-time object detection with region proposal networks," *IEEE Trans. Pattern Anal. Mach. Intell.*, vol. 39, no. 6, pp. 1137–1149, Jun. 2017.
[29] H. Lu *et al.* (2019). "CONet: A cognitive ocean network." [Online]. Available: https://arxiv.org/abs/1901.06253
[30] C. Szegedy *et al.*, "Going deeper with convolutions," in *Proc. IEEE Conf. Comput. Vis. Pattern Recognit.*, Jun. 2015, pp. 1–9.
[31] C. Szegedy, V. Vanhoucke, S. Ioffe, J. Shlens, and Z. Wojna, "Rethinking the inception architecture for computer vision," in *Proc. IEEE Conf. Comput. Vis. Pattern Recognit.*, Jun. 2016, pp. 2818–2826.
[32] M. D. Zeiler and R. Fergus, "Visualizing and understanding convolutional networks," in *Proc. Eur. Conf. Comput. Vis.*, 2014, pp. 818–833.
[33] H. Lu *et al.*, "Wound intensity correction and segmentation with convolutional neural networks," *Concurrency Comput., Pract. Exper.*, vol. 29, no. 6, 2017, Art. no. e3927.
[34] A. Krizhevsky, I. Sutskever, and G. E. Hinton, "ImageNet classification with deep convolutional neural networks," in *Proc. 25th Int. Conf. Neural Inf. Process. Syst.*, 2012, pp. 1097–1105.
[35] K. He, X. Zhang, S. Ren, and J. Sun, "Deep residual learning for image recognition," in *Proc. IEEE Conf. Comput. Vis. Pattern Recognit.*, Jun. 2016, pp. 770–778.
[36] M. Everingham, L. Van Gool, C. K. I. Williams, J. Winn, and A. Zisserman, "The Pascal visual object classes (VOC) challenge," *Int. J. Comput. Vis.*, vol. 88, no. 2, pp. 303–338, Sep. 2009.
[37] C. Y. Fu, W. Liu, A. Ranga, A. Tyagi, and A. C. Berg. (2017). "DSSD: Deconvolutional single shot detector." [Online]. Available: https://arxiv.org/abs/1701.06659
[38] H. Waghmare, R. Kokare, and Y. Dandawate, "Detection and classification of diseases of grape plant using opposite colour local binary pattern feature and machine learning for automated decision support system," in *Proc. 3rd Int. Conf. Signal Process. Integr. Netw.*, Feb. 2016, pp. 513–518.
[39] M. Kulin, T. Kazaz, I. Moerman, and E. De Poorter, "End-to-end learning from spectrum data: A deep learning approach for wireless signal identification in spectrum monitoring applications," *IEEE Access*, vol. 6, pp. 18484–18501, 2018.
[40] Y. Zhang, R. Gravina, H. Lu, M. Villari, and G. Fortino, "Pea: Parallel electrocardiogram-based authentication for smart healthcare systems," *J. Netw. Comput. Appl.*, vol. 117, pp. 10–16, Sep. 2018.
[41] K. P. Ferentinos, "Deep learning models for plant disease detection and diagnosis," *Comput. Electron. Agricult.*, vol. 145, pp. 311–318, Feb. 2018.
[42] A. Ramcharan, K. Baranowski, P. McCloskey, B. Ahmed, J. Legg, and D. P. Hughes, "Deep learning for image-based cassava disease detection," *Frontiers Plant Sci.*, vol. 8, p. 1852, Oct. 2017.
[43] A. Johannes *et al.*, "Automatic plant disease diagnosis using mobile capture devices, applied on a wheat use case," *Comput. Electron. Agricult.*, vol. 138, pp. 200–209, Jun. 2017.

PENG JIANG was born in Zhejiang, in 1997. He is currently pursuing the B.S. degree in electronic commerce from Northwest A&F University, China. His research interests include computer vision, object detection, and deep learning.

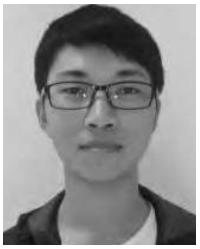

YUEHAN CHEN was born in Guangdong, in 1997. He is currently pursuing the B.S. degree in electronic commerce from Northwest A&F University, China. His research interests include deep learning and computer vision.

BIN LIU was born in Shaanxi, in 1981. He received the B.S. degree in computer science and technology from the Shaanxi University of Science and Technology, China, in 2004, the M.Sc. degree in technology with a major in parallel computing and cloud computing from Yunnan University, China, in 2010, and the Ph.D. degree in electronic and information engineering from Xi'an Jiaotong University, China, in 2014.

Since 2018, he has been an Associate Professor with the College of Information Engineering, Northwest A&F University, China, where he is currently a Postdoctoral Fellow with the College of Mechanical and Electronic Engineering. His research interests include deep learning and computer vision. He currently serves as a Reviewer for the IEEE Access, the IEEE Transactions on Computers, and *The Journal of Supercomputing*, among other journals.

DONGJIAN HE received the B.E., M.E., and D.E. degrees in agricultural engineering from Northwest A&F University, in 1982, 1985, and 1998, respectively. He was a Lecturer with the College of Mechanical and Electronic Engineering, Northwest A&F University, from 1987 to 1992, and an Associate Professor, from 1992 to 1999, where he is currently a Professor. His research interests include computer graphics, image analysis, and machine vision. He is a member of the China Computer Federation, the Chairman of the Shaanxi Society of Image and Graphics, the Vice Chairman of the Electrical Information and Automation Committee of CSAE, and a member of the Council of the Chinese Society for Agricultural Machinery.

CHUNQUAN LIANG received the B.S. degree in computer science and technology and the M.S. degree in computer software and theory from Northwestern Polytechnical University, China, in 2003 and 2006, respectively, and the Ph.D. degree in technology of computer application from Northwest A&F University, in 2014. From 2006 to 2014, he was a Lecturer with the College of Information Engineering, Northwest A&F University. In 2015, he was with the Database Management Group, UNSW, Australia, as an Visiting Academic. Since 2016, he has been an Associate Professor with the College of Information Engineering, Northwest A&F University. He has published many papers in journals and conferences. His research interests include database management and data mining, massive data analysis, and uncertain data mining.